Monatshefte für Chemie 129, 1139–1149 (1998)

Monatshefte für Chemie
Chemical Monthly

Physical Properties of Some New Uranyl Complexes with Ligands Derived from Acetone

Adel S. Orabi

Chemistry Department, Faculty of Science, Suez Canal University, Ismailia, Egypt

Summary. Uranyl complexes with 1,3-diphenyl-1-(2-hydroxy-anilidino)-1-propylidin-3-one (H_2A), 1,3-diphenyl-1-ethanolimine-propylidin-3-one (HB^1), 4-phenyl-2-ethanolimino-2-butylidin-4-one (HB^2), and 2-ethanolimino-2-pentylidin-4-one (HB^3) as ligands were prepared and characterized by elemental analysis, electrical conductivity measurements, magnetic susceptibility determination, mass, IR, and UV/Vis spectroscopy, and thermogravimetry. The complexes can be formulated as $[UO_2L(H_2O)(NO_3)]\cdot nH_2O$ with the exception of UO_2-HB^1 which has to be written as $[UO_2L_2(H_2O)]\cdot nH_2O$. The structures of these complexes were fitted using Alchemy III. The thermogravimetric studies suggest the following order of relative thermal stability of the complexes: UO_2-H_2A>UO_2-HB^1≈UO_2-HB^2>UO_2-HB^3. ΔE_{act} (calculated from the endothermic peaks) of the liberation of H_2O of crystallization increases within the order UO_2-HB^3>UO_2-HB^1>UO_2-HB^2>UO_2-H_2A. The antimicrobial activities of the prepared complexes have been tested.

Keywords. Uranyl complexes; Acetone derivatives; Antimicrobial activity; Thermal stability.

Physikalische Eigenschaften einiger neuer Uranylkomplexe mit Acetonderivaten als Liganden

Zusammenfassung. Uranylkomplexe mit 1,3-Diphenyl-1-(2-hydroxy-anilidino)-1-propylidin-3-on (H_2A), 1,3-Diphenyl-1-ethanolimin-propylidin-3-on (HB^1), 4-Phenyl-2-ethanolimino-2-butylidin-4-on (HB^2) und 2-Ethanolimino-2-pentylidin-4-on (HB^3) als Liganden wurden hergestellt und mittels Elementaranalyse, Konduktivitäts- und Suszeptibilitätsmessungen, Massen-, IR- und UV/Vis-Spektroskopie sowie Thermogravimetrie charakterisiert. Die Komplexe können als $[UO_2L(H_2O)(NO_3)]\cdot nH_2O$ formuliert werden; eine Ausnahme bildet UO_2-HB^1, dem die Formel $[UO_2L_2(H_2O)]\cdot nH_2O$ zugeordnet wird. Die Strukturen der Komplexe wurden mit Hilfe des Programms Alchemy III gefittet. Die thermogravimetrischen Untersuchungen legen die Stabilitätsreihenfolge UO_2-H_2A>UO_2-HB^1≈UO_2-HB^2>UO_2-HB^3 nahe. ΔE_{act} der Freisetzung des Kristallwassers, berechnet aus den endothermen Peaks, steigt in der Reihenfolge UO_2-HB^3>UO_2-HB^1>UO_2-HB^2>UO_2-H_2A. Die antimikrobielle Aktivität der hergestellten Komplexe wurde untersucht.

Introduction

The uranyl ion (UO_2^{2+}) is of great significance due to its versatile applications. Although it is of unusual solubility in organic phases, it is easily extractable from aqueous layers. It shows little or no ionization; nitrate ions are coordinated in equatorial positions of the UO_2 unit [1, 2]. *Schiff* bases derived form β-diketones as well as the uranyl ion have gained much attention because of their biological [3, 4], industrial [5–9], and analytical applications [10–15]. A careful survey of the literature has shown that no systematic work has been done on uranyl complexes with the title compounds. We thought it to be interesting to prepare some uranyl nitrate complexes with these ligands. The structure of the formed complexes was studied by different physicochemical methods; the antimicrobial activities of the complexes were tested.

Results and Discussion

Thermal reactions of uranyl nitrate with the *Schiff* bases H_2A, HB^2, and HB^3, in ethanol-water resulted in the formation of 1:1 (metal:ligand) complexes with the general formula $[UO_2L(H_2O)(NO_3)]\cdot nH_2O$. Reactions of $UO_2(NO_3)_2$ with HB^1, however, gave a 1:2 complex with the molecular formula $[UO_2L_2(H_2O)]\cdot nH_2O$. The complexes were found to be either yellow, orange, deep orange, or olive-green colored non-hygroscopic powders, moderately soluble (up to $\sim 5\times 10^{-2}\,M$) in acetone, methanol, ethanol, *DMF*, *DMSO*, and chloroform. They were insoluble in benzene and petroleum ether. The molar conductances of the complexes in chloroform, acetone, methanol, ethanol, and *DMSO* (Table 1) indicated that all compounds behaved as non-electrolytes [17]. Conductivities increased according to the nature of solvent following the order Acetone >*DMSO* > methanol > ethanol > chloroform, suggesting that the mobility of the complexes has a maximum in acetone and a minimum in chloroform. Hence, we may conclude that acetone is the best extractant for these complexes. Furthermore, the values of conductivity could indicate that the nitrate ion coordinates to the metal ion. All complexes are found to be diamagnetic ($\mu_{\text{eff}} = 0\,\text{BM}$) as expected for a UO_2^{2+} system.

Infrared spectra

The significant IR data of the ligands as well as those of their uranyl complexes are listed in Table 2. The band at 3300–3600 cm^{-1} which is present in all complexes as a weak or a medium broad band may be due to coordinated water molecules. Ligands bands at 3100–3370 cm^{-1} were assigned as $\upsilon_{\text{O-H}}$ and $\upsilon_{\text{N-H}}$ [16]. These bands exerted shifts of ~50–70 cm^{-1} to lower frequencies for complexes **1**, **2**, **5**, and **6**, whereas they were completely absent in complexes **3**, **4**, **7**, and **8**. The bands at 1600 and 1560 cm^{-1} were assigned to $\upsilon_{\text{C=N}}$ and $\upsilon_{\text{C=C}}$; they also displayed slightly negative shift upon complexation. This may result from two opposing factors: (1) coordination at C=N would cause a shift to lower frequencies, and (2) the breaking of intramolecular hydrogen bonds (from the keto-enol equilibrium of the ligand) would cause a shift to higher frequencies. The slightly negative shift indicates that the carbonyl oxygen and the azomethine nitrogen atoms are involved in coordination; the coordination by the metal ion lowers the wavenumber more than hydrogen bonding [18]. On the other hand, the vibrational bands at 3220–3370 cm^{-1} which were assigned to $\upsilon_{\text{O-H}}$ and $\upsilon_{\text{N-H}}$ in the free ligand disappeared or became very weak with a slight negative shift upon complexation. This may indicate that the phenolic oxygen in H_2A or the alcoholic oxygen in HB^1, HB^2, and HB^3 are involved in coordination. Strong absorption in the 933–911 cm^{-1} region

Table 1. Analytical data, effect of temperature, colours and molar conductivities of the synthesized complexes in different solvents

		Molecular weight	Colour	m.p. (°C)	C (%)		H (%)		N (%)		Conductivity $\times 10^6$ ($ohm^{-1} \cdot cm^2 \cdot mol^{-1}$)				
					calcd.	found	calcd.	found	calcd.	found	*DMSO*	MeOH	EtOH	Acetone	$CHCl_3$
1	$[UO_2H\mathit{A}(H_2O)(NO_3)] \cdot 2H_2O$	700.46	Oily green	270	36.01	35.98	3.17	3.13	4.00	4.02	15	11	3	23	0.06
2	$[UO_2H\mathit{A}(H_2O)(NO_3)]$	664.46	Deep green	268	37.96	37.78	3.74	3.70	4.21	4.11	–	–	–	–	–
3	$[UO_2\mathit{B}^1_2(H_2O)] \cdot H_2O$	838.73	Orange	200	48.69	48.60	4.34	4.29	3.34	3.26	16.5	15	6.1	28.5	0.06
4	$[UO_2\mathit{B}^1_2(H_2O)]$	820.73	Brown	203	49.75	49.56	4.18	4.20	3.41	3.35	–	–	–	–	–
5	$[UO_2\mathit{B}^2(H_2O)(NO_3)] \cdot 1/2H_2O$	563.32	Orange	108	25.58	25.39	3.05	3.12	4.97	4.89	22.5	26.5	12	40	0.08
6	$[UO_2\mathit{B}^2(H_2O)(NO_3)]$	554.32	Deep brown	115	26.00	26.04	2.92	2.97	5.05	5.07	–	–	–	–	–
7	$[UO_2\mathit{B}^3(H_2O)(NO_3)] \cdot H_2O$	510.26	Yellow	> 300	16.48	16.36	3.17	3.12	5.49	5.60	16	11	3.6	24	0.06
8	$[UO_2\mathit{B}^3(H_2O)NO_3)]$	492.26	Orange	> 300	17.08	16.98	2.87	2.78	5.69	5.64	–	–	–	–	–

Table 2. IR (KBr) and UV/Vis (ethanol) spectroscopic data

		IR (cm^{-1})								UV/Vis (nm)			
		υ_{H_2O}	υ_{O-H} υ_{N-H}	$\upsilon_{C=N}$	υ_{M-O}	υ_{M-N}	υ_4 (NO_3)	υ_1 (NO_3)	υ_3 (O=U=O)				
	H_2A	–	3370 (s) 3310 (s)	1600 (s) 1560 (s)	–	–	–	–	–	340 (s)	280 (s)	230 (sh)	
1	$[UO_2HA(H_2O)(NO_3)]\cdot 2H_2O$	3300–3600 (br)	3310 (w) 3250 (w)	1602 (s) 1554 (s)	520 (m)	418 (m)	1517 (s)	1360	912 (s)	385 (s)	325 (s)	260 (sh)	
2	$[UO_2HA(H_2O)(NO_3)]$	3500 (vw)	3326 (w) 3240 (w)	1601 (m) 1552 (m)	530 (w)	418 (vw)	1519 (m)	1367	913 (s)	390 (sh)	330 (sh)	280 (m)	250 (sh)
	HB^1	–	3310 (m, br)	1590 (s) 1550 (s) 1530 (m)	–	–	–	–	–	345 (s)	245 (s)		
3	$[UO_2B^1_2(H_2O)]\cdot H_2O$	3500 (br)	–	1578 (s) 1520 (s)	528 (m)	428 (w)	–	–	911 (s)	390 (sh)	330 (s)	255 (s)	
4	$[UO_2B^1_2(H_2O)]$	3500 (w, br)	–	1589 (s) 1517 (s)	528 (m)	450 (w)	–	–	933 (s)	390 (sh-w)	330 (s)	255 (s)	
	HB^2	–	3350 (s)	1600 (s) 1590 (s)	–	–	–	–	–	335 (s)	235 (s)		
5	$[UO_2B^2(H_2O)(NO_3)]\cdot 1/2H_2O$	3500 (br)	3220 (br)	1600 (s) 1555 (m)	517 (m)	420 (vw)	1533 (m)	1278 (s)	933 (s)	370 (sh)	300 (s)	250 (sh)	
6	$[UO_2B^2(H_2O)(NO_3)]$	3411 (br)	3130 (w)	1589 (m)	528 (m)	422 (m)	1533 (w)	–	917 (s)	365 (sh)	300 (s)	245 (s)	210 (s)
	HB^3	–	3270 (s)	1600 (s) 1550 (s)	–	–	–	–	–	305 (s)			
7	$[UO_2B^3(H_2O)(NO_3)]\cdot H_2O$	3320 (br)	– –	1586 (w) 1570 (w)	533 (m)	411 (s)	1520 (s)	1267 (s)	928 (s)	350 (sh)	275 (s)		
8	$[UO_2B^3(H_2O)(NO_3)]$	3420 (w, br)	–	1588 (m) 1570 (w)	528 (w)	411 (w)	1522 (s)	1256 (m)	928 (s)	350 (sh)	275 (s)		

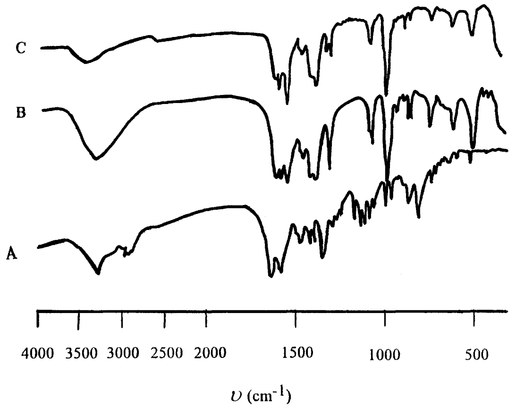

Fig. 1. IR spectra of HB^3 and its uranyl complexes; A = HB^3, B = UO_2-HB^3, C = UO_2-HB^3 after heating at 100°C for 2 h

were assigned to an asymmetric stretching vibration (υ_3) of the O=U=O moiety. Also, the appearance of a υ_{M-O} band at 517–530 cm^{-1} and υ_{M-N} at 411–450 cm^{-1} supports chelation through the N and O atoms. These bands gave positive shifts after partially dehydration of the complexes (Table 2, Fig. 1) due to increasing *Lewis* acidity of the central atom [19]. The bands around 1520 and 1300 cm^{-1} in **1**, **2**, and **5**–**8** were attributed to the two split bands of the coordinated NO_3 ion. The magnitude of splitting in the order of about 150 cm^{-1} in **1** and **2** indicated that NO_3 coordinated to the central metal as a monodentate ligand [20], whereas the splitting in the order of about 255 cm^{-1} in the other complexes suggested a bidentate coordination of the nitrate ions [20].

Electronic spectra

The electronic spectra of the uranyl complexes showed bands in the region of 350–390 nm which could not be observed in the complexing agent; these are due to the uranyl group (Fig. 2) [21–23]. This band was strongly affected by the nature of the complexing agent. Ligands with extended conjugation shift this band to longer wavelengths. The uranyl complex **1** gave two further bands at 325 and 260 nm, corresponding to the complexing moiety. They were assigned to the $\pi \longrightarrow \pi^*$ transition of the keto-enol isomers of the ligand (340 and 280 nm) and exerted blue shifts relative to those of the ligands *i.e.* the conjugation became somewhat restricted upon complexation. The longer wavelength band may be due to the enol form which permits continuous conjugation. The same behavior was observed for the other complexes with slight deviations observed in the shorter wavelength band which exhibited red shifts. In these complexes, the conjugation of the keto isomer might become somewhat more effective upon complexation [24–27] (Table 2). The removal of water of crystallization gave no change in the band positions.

Thermal analyses

The thermogravimetric studies of the complexes gave more insight on their molecular structure. The thermalgravimetric curves of the complexes (see Fig. 3

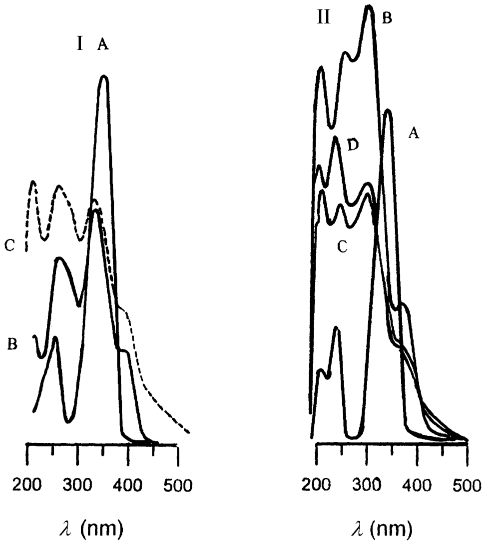

Fig. 2. UV/Vis spectroscopic bands for some ligands and complexes; I: A = HB^1, B = UO_2-HB^1, C = UO_2-HB^1 after heating at 168°C for 2 h; (II) A = HB^2, B = UO_2-HB^2, C = UO_2-HB^2 after heating at 98°C for 2 h, D = UO_2-HB^2 after heating at 132°C for 2 h

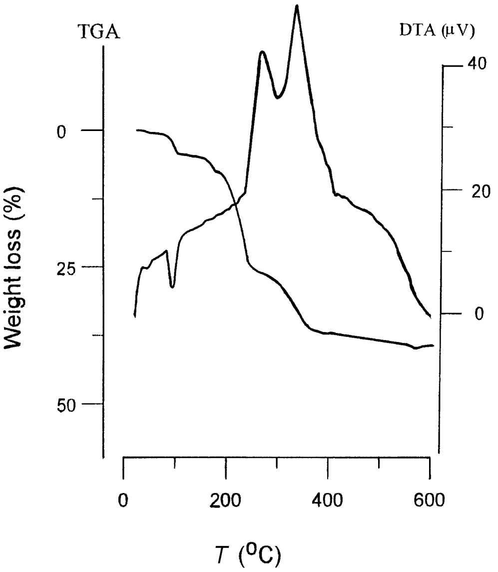

Fig. 3. DTA and TGA diagram for UO^2-HB^3

for an example) showed that complexes (**1**, **3**, **6**, and **7**) exhibited a well-defined endothermic peak in the temperature range of 80–115°C. This could be probably due to the liberation of water of crystallization [28]. The second stage of the decomposed product appeared at a temperature range of 130–170°C as endothermic changes which may be due to coordinated water [29]. Such a peak is not observed in the DTA thermograms for complexes **3** and **7**, however the

Table 3. Thermal analysis data

	T (°C)	Weight loss (%)		ΔE (kJ $\cdot$ mol^{-1})	Assignment
		Found	Calculated		
1 $[\mathrm{UO_2H}A(\mathrm{H_2O})(\mathrm{NO_3})]\cdot 2\mathrm{H_2O}$	80	5.04	5.14	61.41 (endo)	hydrated H_2O
	170	2.26	2.57	–	coordinated H_2O
	297	–	44.88	1517.0 (endo)	ligand decomposition
	333	–		146.33 (endo)	ligand decomposition
3 $[\mathrm{UO_2}B^1_2(\mathrm{H_2O})]\cdot \mathrm{H_2O}$	115	2.01	2.15	110.46 (endo)	hydrated H_2O
	155	1.99	2.15	–	coordinated H_2O
	295	0.0	–	–	phase transition
	300	63.24	63.51	244.56 (exo)	ligand decomposition
5 $[\mathrm{UO_2}B^2(\mathrm{H_2O})(\mathrm{NO_3})]\cdot 1/2\mathrm{H_2O}$	98	1.56	1.60	83.79 (endo)	hydrated H_2O
	130	3.08	3.20	139.81 (endo)	coordinated H_2O
	215	36.17	36.44	126.66 (exo)	ligand decomposition
	503	–	11.01	172.37 (exo)	NO_3 liberation
7 $[\mathrm{UO_2}B^3(\mathrm{H_2O})(\mathrm{NO_3})]\cdot \mathrm{H_2O}$	97	3.46	3.53	208.27 (endo)	hydrated H_2O
	130	3.31	3.53	–	coordinated H_2O
	274	28.04	28.06	153.94 (exo)	ligand decomposition
	341			145.67	ligand decomposition

change was well observed in the TG curves. The decomposition of the complexing agent started at ~295°C for complexes **1** and **3** and at 215 and 274°C for complexes **5** and **7**. From the TG diagram, the weight loss supports the formulae listed in Table 1. The obtained results suggest the following thermal stability order of the different species:

(a) thermal stability of the water of crystallization: **3** > **5** > **7** > **1**;
(b) thermal stability of the coordinated water: **1** > **3** > **5** ≈ **7**; and
(c) thermal stability of the complexing agent: **1** > **3** > **7** > **5**.

The stability of the coordinated water molecules in their uranyl complexes increased with increasing conjugation in the complexing agent, *i.e.* $\mathrm{H_2}A > \mathrm{H}B^1 > \mathrm{H}B^2 > \mathrm{H}B^3$. The high stability of the complexes derived from $\mathrm{H_2}A$ might be due to the unsaturated orbitals of this ligand which overlap with the unsaturated orbitals of the uranyl ion, thus increasing the *Lewis* acidity of that ion and rendering the bond between the ion and the *Lewis* base (H_2O, NO_3 or organic ligand) more stable. The activation energies of the thermal decomposition steps have been calculated from the data obtained from the DTA thermograms using the *Piloyan* method [30] (Table 3). It is worth mentioning that E_{act} of decomposition of the complexing agent in the uranyl complexes has the order **1** > **3** > **5** > **7** which also agrees with the extent of the conjugation. These results are consistent with those obtained from UV/Vis spectroscopy.

Mass spectra

The structure of the ligands was elucidated from their mass spectroscopic data (Table 4). As an example, the fragmentation of $\mathrm{H}B^3$ is shown in Scheme 1.

Table 4. Mass spectra of the ligands and their uranyl complexes

	m/*z* (%)
A	315 (20), 253 (30), 238 (15), 220 (10), 196 (8), 176 (12), 160 (5), 148 (15), 134 (100), 120 (15), 109 (18), 105 (80), 93 (10), 77 (55), 65 (15), 51 (16), 39 (15)
B^1	267 (15), 223 (100), 178 (5), 147 (48), 118 (5), 105 (47), 89 (8), 77 (49), 69 (65), 65 (5), 51 (20), 39 (5)
B^2	205 (54), 188 (20), 174 (53), 162 (40), 145 (10), 133 (10), 128 (15), 115 (10), 110 (7), 105 (98), 91 (100), 82 (30), 77 (60), 69 (5), 68 (5), 67 (5), 55 (10), 51 (15), 42 (30), 30 (10)
B^3	143 (65), 128 (35), 112 (75), 100 (40), 94 (41), 84 (43), 82 (45), 70 (32), 58 (26), 55 (28), 43 (100), 39 (30), 30 (65), 27 (25)
UO_2-*A*	664 (8), 646 (10), 598 (7), 584 (8), 493 (8), 404 (6), 324 (5), 297 (15), 270 (12), 223 (65), 195 (25), 147 (40), 109 (40), 105 (100), 77 (85), 69 (55), 51 (35)
UO_2-B^1	820 (10), 804 (10), 717 (55), 700 (5), 600 (25), 554 (5), 522 (6), 493 (35), 476 (5), 428 (5), 416 (15), 287 (5), 270 (60), 224 (20), 207 (12), 191 (25), 105 (100), 77 (70), 69 (25), 51 (13)
UO_2-B^2	555 (5), 536 (6), 473 (3), 431 (12), 354 (5), 303 (6), 286 (2), 270 (22), 162 (25), 147 (25), 120 (25), 105 (100), 77 (85), 69 (25), 51 (60), 43 (63), 27 (10)
UO_2-B^3	492 (7), 474 (7), 468 (50), 453 (15), 426 (15), 412 (12), 398 (10), 369 (100), 354 (22), 351 (10), 298 (8), 287 (10), 270 (80), 98 (15), 85 (15), 67 (15), 43 (35)

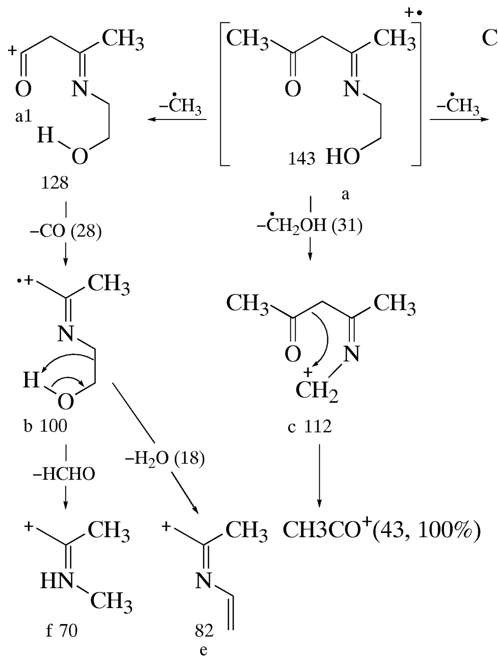

Scheme 1. Postulated fragments of HB^3

The mass spectrum of the HB^3-uranyl complex showed that the two molecules of water derived from the elemental analysis are not water of crystallization. One of them is coordinated with the metal and included in its molecular weight as confirmed by the loss of one molecule of water from the molecular ion peak

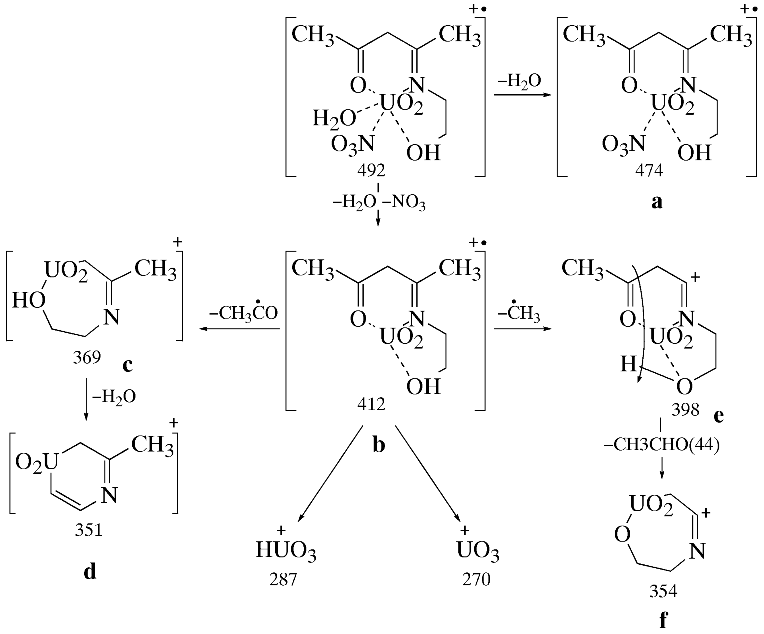

Scheme 2. Postulated fragments of the HB^3-uranyl complex

(Table 4, Scheme 2) at $m/z = 492$ (7%) to give the radical cation (a) with $m/z = 474$ (7%) which in turn loses NO_3 to give the radical cation (b) with $m/z = 412$ (12%) from which all further fragmentation takes place. The loss of an acetyl radical left the cation $m/z = 369$ (100%) which lost one molecule of water to give a cation (d) with $m/z = 351$ (10%). The uranium oxide cation appeared at $m/z = 270$ (80%), HUO_3 at $m/z = 287$ (10%). The loss of a methyl group from (b) gave the cation at $m/z = 298$ (8%) which extruded acetaldehyde to give cation (f) at $m/z = 354$ (22%).

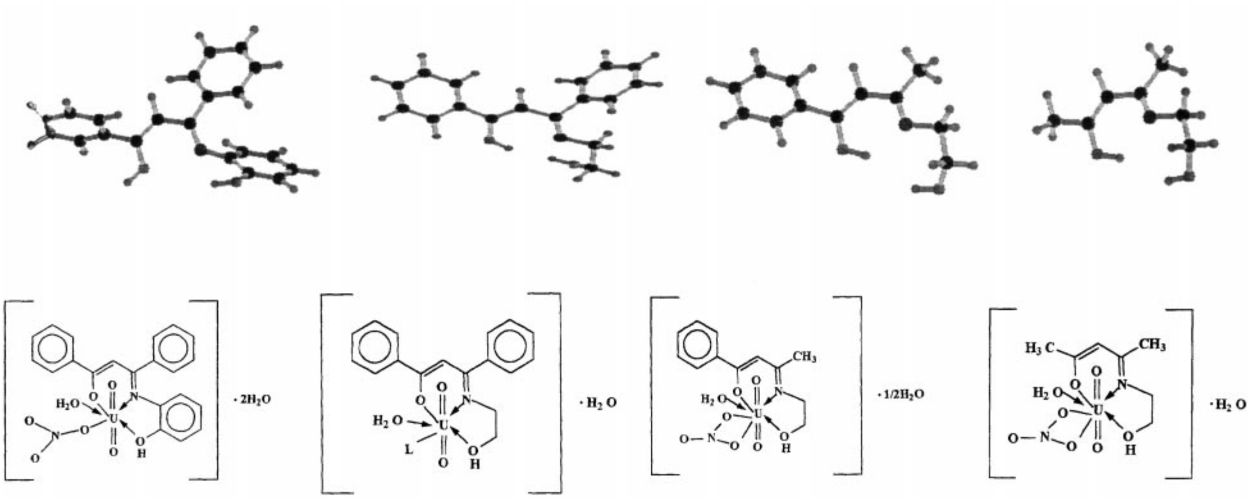

Scheme 3. Molecular modeling of the ligands and postulated structure of the uranyl complexes

Antibiological activities

There were no clear zones around all wells of different concentrations of tested drugs. The drugs are considered ineffective at all used concentrations.

Molecular modeling

The postulated spatial arrangements have been confirmed using the molecular modeling program Alchemy III. The program has been applied on many different arrangements for each ligand, the most stable one (which gave the minimum molecular energy) being presented in Scheme 3.

Experimental

Reagents

Uranyl nitrate (AnalaR, 99.9% pure) was purchased form BDH. All organic solvents were of analytical grade and purified by standard methods. The *Schiff* base ligands 1,3-diphenyl-1-(2-hydroxy-anilidino)-1-propylidin-3-one (H_2A), 1,3-diphenyl-1-ethanolimine-propylidin-3-one (HB^1), 4-phenyl-2-ethanolimino-2-butylidin-4-one (HB^2), and 2-ethanolimino-2-pentylidin-4-one (HB^3) were prepared as described previously [16].

Syntheses

$0.02\,M$ of ethanolic *Schiff* base solution and $0.01\,M$ UO_2 nitrate solution (ethanol-water mixture) were mixed and heated to reflux for 2–3 h. Yellowish-orange complexes were formed in cases of HB^1, HB^2 and HB^3 whereas olive-green crystals were obtained from H_2A after recrystallization from hot ethanol. The crystals were dried *in vacuo* for a few hours. The purities of the complexes were checked by measurement of their melting points and TLC (silica gel GF254 type 60, mesh size 50–250, eluted with ethanol-chloroform).

The antibiological activities were measured by the hole diffusion method. Five mm wells were made in *Czapek*'s agar medium using a stainless steel cork borer. The wells were filled with different concentrations of the tested substances (100 and 1000 ppm). The medium was seeded with propagules of either *Fusarium oxysporum* or *Rhizoctonia solani* as testing microorganisms (fungi). The drug is considered effective if it inhibits the growth of the testing microorganism. This was determined by the clear zone shown around the wells. Wells containing either solvent alone or distilled water served as a control.

Equipment

Infrared spectra were recorded in the range of $4000-400\,cm^{-1}$ (KBr discs) on a Perkin-Elmer 883 spectrophotometer. Elemental analyses were carried out using a Heraeus CHN Rapid Analyzer. Thermal analyses of the complexes under investigation were carried out on a STA 409 Netzsch Simultaneous thermoanalyzer. UV/Vis spectra were measured at room temperature on a Beckman model 5260 spectrophotometer in 1 cm quartz cells. The conductance measurements of $1\times10^{-3}M$ solutions of the complexes in different solvents were performed using a WTW model LF-42 conductivity bridge fitted with an LTA-100 conductivity cell. The spatial structures were fitted using the alchemy III chemical modeling program. Mass spectra of the complexes were obtained with a mass spectrometer Varian MAT 711. Magnetic susceptibilities of the complexes were measured on a Bruker Magnet B–E 15 instrument.

References

[1] Cotton FA, Wilkinson G (1972) Advanced Inorganic Chemistry, 3rd edn. Wiley, New York

[2] Sobhana G, Indrasenan P (1987) Inorg Chim Acta **133**: 157

[3] Kaim W, Schwederski B (1996) Bioinorganic Chemistry: Inorganic Elements in the Chemistry of Life. Wiley, New York

[4] Das AK (1990) A Text Book on Medicinal Aspects of Bio-Inorganic Chemistry. CBS, India

[5] Munoz JA, Ballester A, Gonzalez F, Blazquez ML (1995) Hydrometallurgy **38**: 59

[6] Yanase N, Sekine K (1995) Materials Research Society Symposium Proceedings, Pittsburgh, No. 353, p 2

[7] Bruno J, Casas I, Cera E, Ewing RC, Finch RJ, Werme LO (1995) Materials Research Society Symposium Proceedings, Pittsburgh, No. 353, p 1

[8] Steffey BD, Miedaner A, Maciejewski-Farmer ML, Bernatis PR, Herring AM, Allured VS, Carperos V, DuBois DL (1994) Organometallics **13**: 4844

[9] Syamal A, Singh MM (1994) Reactive Polymers **24**: 27

[10] Hines K, Theriot LJ (1991) Synth React Inorg Met-Org Chem **21**(**1**): 89

[11] Sievers RE, Eisentraut KJ, Griest DJ, Richardson MF, Wolf WR, Ross WD, Frew NM, Isenhour TL (1971) Second Lunar Science Conf **2**: 1451

[12] Ross WD, Scribner WG, Sievers RE (1970) 8th Int Symp on Gas Chromatography 369

[13] Mushak D, Glenn MT, Savory J (1973) Fluorine Chem Rev **6**: 116

[14] Rodriguez-Vazquez JA (1974) Anal Chim Acta **1**: 73

[15] Sali SK, Kulkami NK, Sampath S, Jayadevan NC (1994) Journal of Nuclear Materials **217**: 294

[16] Ibrahim ES, Sallam SA, Orabi AS, El-Shetary BA, Lentz A (1998) Monatsh Chem **129**: 159

[17] Geary WJ (1971) Coord Chem Rev **7**: 81

[18] Lal Ram A, Singh MN, Das S (1986) Synth React Inorg Met-Org Chem **16**(**4**): 513

[19] Nakamoto K (1986) Infrared and Raman Spectra of Inorganic and Coordination Compound. 4th edn. Wiley, New York

[20] Curtis NF, Curtis YM (1965) Inorg Chem **4**: 804

[21] Basu G, Belford RL (1966) J Inorg Nucl Chem **28**: 252

[22] Rabinowitch E, Belford RL (1964) Spectroscopy and Photochemistry of Uranyl Compounds. Pergamon, Oxford

[23] Sacconi L, Giannoni G (1954) J Chem Soc 2751

[24] El-Sonbati AZ (1991) Synth React Inorg Met-Org Chem **21**: 1469

[25] Casellato U, Vidali M, Vigato A (1976) Inorg Chim Acta **18**: 77

[26] McGlynn SP, Smith JK (1961) J Mol Spec **6**: 164

[27] Rao CNR (1975) Ultra-Violet and Visible Spectroscopy Chemistry Applications. Butterworth, London

[28] Rakha TH, El-Asmy AA, Mostafa MM, El-Kourshy A (1987) Trans Met Chem **12**: 125

[29] Proceedings of the Sixth International Conference in Thermal Analysis (1980) Bayreuth, Germany

[30] Piloyan GO, Ryabchikov ID, Novikova OS (1966) Nature **212**: 1229

Received March 10, 1998. Accepted (revised) June 9, 1998